

Perturbation theory for solid–liquid interfacial free energies

Vadim B Warshavsky and Xueyu Song

Ames Laboratory and Department of Chemistry, Iowa State University, Ames, IA 50011, USA

E-mail: xsong@iastate.edu

Received 17 February 2010, in final form 19 March 2010

Published 20 August 2010

Online at stacks.iop.org/JPhysCM/22/364112

Abstract

A perturbation theory is developed to calculate solid–liquid interfacial free energies, including anisotropy. The method is applied to systems with inverse-power and Lennard-Jones pair potentials as well as to metal systems with embedded-atom model potentials. The results are in reasonable agreement with the corresponding ones obtained from molecular dynamics simulations.

1. Introduction

The crystal–melt interfacial free energy γ is the reversible work needed to form a unit area of interface between a crystal and its melt. The parameter γ is critically important when the kinetics and morphology of crystal growth are studied, because the magnitude of γ is one of the crucial quantities governing the nucleation rate of crystals, whereas its anisotropy plays a fundamental role during dendritic growth (see reviews [2, 1, 3, 4]).

The thermodynamic theory of a solid–liquid interface was developed by Gibbs [5] initially and later refined by many authors (for recent developments see [6–9]). Given the difficulties of experimentally measuring γ , especially γ s anisotropy, theoretical and computational methods provide an attractive alternative to understand the thermodynamics of solid–liquid interfaces from the molecular point of view.

There are two main approaches for the calculation of γ using molecular simulations: the cleaving method [10, 11] and the fluctuation method [12]. These methods have been applied to the calculation of γ for simple model systems such as hard-spheres (HS) [11, 13, 14], hard-sphere mixtures [15], soft-spheres (SS) [18], Lennard-Jones (LJ) [10, 19, 20, 17, 7] and LJ mixtures [21], as well as more realistic models, particularly anisotropic hard-dumbbells [16], metals [12, 22, 23] and metal alloys [24] and water models [25]. In spite of the remarkable progress in computational power, such simulations are still quite demanding, especially for alloys or other multi-component systems.

Thermodynamic perturbation theory has been shown to yield reliable and accurate bulk thermodynamic properties for many model and realistic systems [31, 53]. Naturally an

extension of the perturbation theory to the interfacial properties between liquid and solid phases can be developed. For the liquid–vapor surface tension case, there have been some attempts [26–28], but it is expected that the perturbation theory may not work well because a thermodynamic perturbation approach, which is mean field in nature, is not suitable even for the bulk vapor phase. Some ad hoc perturbation methods have been employed to estimate the solid–liquid interfacial free energy of LJ systems [29, 30]. In the current study we present a rigorous approach to calculate γ (including its anisotropy) based on the thermodynamical perturbation theory of Weeks, Chandler and Anderson (WCA) [31]. As a reference system, we chose a HS model, because it exhibits a liquid–solid interface, and its interfacial free energy values are well documented. Using our approach, interfacial free energies of inverse-power and LJ systems are in good agreement with the results from MD simulations. Applications of our theory to model metallic systems also show that our perturbation theory can provide a useful way to compute interfacial free energies of a variety of systems just like the widely used perturbation theory for bulk properties.

The rest of the paper is organized as follows. The perturbation theory for the solid–liquid interfacial free energy is described in section 2. The results are presented in section 3. The discussion and conclusions are given in section 4. Some details of derivations are given in the appendices.

2. Theory

Consider a one-component system consisting of N particles in the volume V at temperature T with a coexistence between liquid and solid phases. Let the z axis be normal to the

interface, $z < z_0$ corresponds to the solid phase, $z > z_0 + \Delta z$ to the liquid phase and Δz is the thickness of the interfacial region.

The bulk density of the liquid phase is ρ^l and the number density in the bulk solid phase is an inhomogeneous function $\rho^s(\vec{r})$, which is commonly parameterized by a sum of normalized Gaussian distributions around its lattice sites. In the solid–liquid interfacial region the density $\rho(\vec{r})$ could be parameterized in a similar way such that the width of density peaks increases as the interfacial layer changes from the solid to liquid phase [32]. A smoothed or volume-averaged density is often introduced for the bulk solid phase $\rho^s = \frac{1}{V} \int d\vec{r} \rho^s(\vec{r})$, which is the bulk density of the solid phase. For the solid–liquid interface a layer-averaged density $\bar{\rho}(z) = \frac{1}{A} \int \int \rho(\vec{r}) dx dy$ [33] can be introduced to characterize the density change in the interfacial region, with A the area of the cross section of the interface. It is typically approximated by a hyperbolic tangent function [32], which is well supported by simulation results for various systems [33]

$$\bar{\rho}(z) = \rho^l + [\rho^s - \rho^l]\Theta(z), \quad (1)$$

where

$$\Theta(z) = \begin{cases} 1, & |z| \leq z_0 \\ \frac{1}{2} \left(1 - \tanh \left(\frac{6(z - z_0 - \Delta z/2)}{\Delta z} \right) \right), & z_0 < |z| \leq z_0 + \Delta z \\ 0, & z_0 + \Delta z < z. \end{cases} \quad (2)$$

The interfacial free energy γ is defined as

$$\gamma A = \Omega + PV = F - \mu N + PV,$$

where Ω and F are the grand canonical potential and Helmholtz free energy for the whole system and P and μ are the pressure and chemical potential of the coexisting bulk phases. Using the thermodynamic relation for the homogeneous phases

$$\mu = f + P/\rho \quad (3)$$

($f = F/N$ is a free energy per particle in the bulk), after the cancellation of the contributions from the bulk phases, we have

$$\gamma A = F^i - \mu N^i + PV^i, \quad (4)$$

where F^i , V^i , N^i are the free energy, volume and number of particles in the interface region. The latter can be found from equation (1) as

$$N^i = \int_{V^i} \rho(\vec{r}) d\vec{r} = A \int_{z_0}^{z_0 + \Delta z} \bar{\rho}(z) dz = \frac{1}{2}(\rho^s + \rho^l)V^i. \quad (5)$$

To transform the right-hand side of equation (4), we write the pressure P in the last term as $\frac{1}{2}(\frac{P}{\rho^s}\rho^s + \frac{P}{\rho^l}\rho^l)$ and substitute equations (3) and (5) into equation (4); we found

$$\gamma A = F^i - \frac{1}{2}(f^s \rho^s + f^l \rho^l)V^i, \quad (6)$$

where $f^s = f^s(\rho^s)$ and $f^l = f^l(\rho^l)$ are the free energies per particle of the coexisting solid and liquid phases.

To calculate the right-hand side of equation (6) we need to know the dependence of F^i , f^s and f^l on the interaction potential of the system. When a pair potential of interaction $\psi(r)$ is given, the Helmholtz free energy of the interfacial region, F^i , can be calculated using the Weeks, Chandler and Anderson (WCA) perturbation approach [31, 34]. Within this approach the interaction potential $\psi(r)$ is separated into a short-range, purely repulsive reference part $\psi_{\text{ref}}(r)$ and a perturbative part $\psi_{\text{pert}}(r)$; the reference system is mapped onto an effective HS system with a temperature-dependent HS diameter d prescribed by the WCA criterion [31, 34, 35]. The resulting expression for the total Helmholtz free energy is

$$F^i = F_{\text{hs},r}^i + F_1^i, \quad (7)$$

where $F_{\text{hs},r}$ is the HS free energy and F_1 is the perturbative part of the free energy [37, 38]

$$F_1^i = \frac{1}{2} \int \int d\vec{r}_1 d\vec{r}_2 \rho(\vec{r}_1) \rho(\vec{r}_2) g_{\text{hs}}(\vec{r}_1, \vec{r}_2) \psi_{\text{pert}}(\vec{r}_1, \vec{r}_2), \quad (8)$$

where g_{hs} is the correlation function of the HS reference system in the interfacial region.

For a homogeneous phase equation (7) the free energy per particle $f = \frac{F}{N}$ is reduced to

$$f = f_{\text{hs},r} + f_1, \quad (9)$$

where the perturbative contribution f_1 is given by

$$f_1 = \frac{1}{2} \rho \int d\vec{r} \bar{g}_{\text{hs}}(r/d) \psi_{\text{pert}}(r), \quad (10)$$

where $\bar{g}_{\text{hs}}(r)$ is the orientationally averaged correlation function [37, 39, 40], $r = |\vec{r}_1 - \vec{r}_2|$.

The main purpose of the present study is to obtain a perturbation formula for γ , i.e. to express γ via the interfacial free energy of the HS solid–liquid system γ_{hs} . To this end we write the counterpart of the expression in equation (6) for the HS solid–liquid system as

$$\gamma_{\text{hs}} A = F_{\text{hs}}^i - \frac{1}{2}(f_{\text{hs}}^s \rho_{\text{hs}}^s + f_{\text{hs}}^l \rho_{\text{hs}}^l) V_{\text{hs}}^i, \quad (11)$$

where ρ_{hs}^s and ρ_{hs}^l are the coexisting HS solid and liquid densities, $f_{\text{hs}}^s = f_{\text{hs}}^s(\rho_{\text{hs}}^s)$ and $f_{\text{hs}}^l = f_{\text{hs}}^l(\rho_{\text{hs}}^l)$ are the corresponding HS solid and liquid free energies per particle; V_{hs}^i is the volume of the HS solid–liquid interface region. The equilibrium HS averaged density profile $\bar{\rho}_{\text{hs}}(z)$ in the interfacial region can be approximated by an expression similar to equation (1)

$$\bar{\rho}_{\text{hs}}(z) = \rho_{\text{hs}}^l + (\rho_{\text{hs}}^s - \rho_{\text{hs}}^l)\Theta(z), \quad (12)$$

where the function $\Theta(z)$ is defined by equation (2) given the width of the HS interfacial region $\Delta z_{\text{hs}} = V_{\text{hs}}^i/A$. Possible ways to find Δz_{hs} as a function of the number of interfacial layers for different orientations of the interface can be found in [32]. From many simulations of various potentials, including the HS system, it is reasonable to assume that

$$V^i \approx V_{\text{hs}}^i. \quad (13)$$

Subtracting equation (11) from (6) and using equation (7), we have

$$\gamma A - \gamma_{\text{hs}} A = F_{\text{hs},r}^i + F_1^i - F_{\text{hs}}^i - \frac{1}{2}(f^s \rho^s + f^l \rho^l - f_{\text{hs}}^s \rho_{\text{hs}}^s - f_{\text{hs}}^l \rho_{\text{hs}}^l) V_{\text{hs}}^i \quad (14)$$

To find the difference $F_{\text{hs},r}^i - F_{\text{hs}}^i = F_{\text{hs}}[\rho(\vec{r})] - F_{\text{hs}}[\rho_{\text{hs}}(\vec{r})]$ in the rhs of equation (14), $F_{\text{hs}}[\rho(\vec{r})]$ can be written as [36]

$$F_{\text{hs}}[\rho(\vec{r})] = k_B T \int d\vec{r} \rho(\vec{r}) (\log[\rho(\vec{r}) \Lambda^3] - 1) + F_{\text{hs}}^{(\text{ex})}[\rho(\vec{r})], \quad (15)$$

where the first part of the right-hand side of equation (15) is the ideal-gas contribution. Λ is the de Broglie wavelength, k_B is the Boltzmann constant and $F_{\text{hs}}^{(\text{ex})}$ is the excess part of the HS free energy. The latter can be expanded as [38]

$$\begin{aligned} F_{\text{hs}}^{(\text{ex})}[\rho(\vec{r})] &= F_{\text{hs}}^{(\text{ex})}[\rho_{\text{hs}}(\vec{r})] \\ &+ \int d\vec{r} \frac{\delta F_{\text{hs}}^{(\text{ex})}}{\delta \rho(\vec{r})} \Big|_{\rho(\vec{r})=\rho_{\text{hs}}(\vec{r})} [\rho(\vec{r}) - \rho_{\text{hs}}(\vec{r})] \\ &+ \frac{1}{2!} \int d\vec{r}_1 d\vec{r}_2 \frac{\delta^2 F_{\text{hs}}^{(\text{ex})}}{\delta \rho(\vec{r}_1) \delta \rho(\vec{r}_2)} \Big|_{\rho(\vec{r})=\rho_{\text{hs}}(\vec{r})} \\ &\times [\rho(\vec{r}_1) - \rho_{\text{hs}}(\vec{r}_1)][\rho(\vec{r}_2) - \rho_{\text{hs}}(\vec{r}_2)] + \dots \end{aligned} \quad (16)$$

Using the definitions of the direct correlation functions [36, 38]

$$c^{(1)}(\vec{r}) = -\beta \frac{\delta F^{(\text{ex})}}{\delta \rho(\vec{r})}, \quad c^{(2)}(\vec{r}, \vec{r}') = -\beta \frac{\delta^2 F^{(\text{ex})}}{\delta \rho(\vec{r}) \delta \rho(\vec{r}')}, \quad (17)$$

as well as the expression for the chemical potential of the HS system $\mu_{\text{hs}} = k_B T \ln[\rho_{\text{hs}}(\vec{r}) \Lambda^3] - \frac{1}{\beta} c^{(1)}(\vec{r})$, a combination of equations (15)–(17) yields

$$F_{\text{hs},r}^i - F_{\text{hs}}^i = F_2^i + (\mu_{\text{hs}} - k_B T) \int d\vec{r} (\rho(\vec{r}) - \rho_{\text{hs}}(\vec{r})) + F_3^i, \quad (18)$$

where

$$F_2^i = k_B T \int d\vec{r} \rho(\vec{r}) \log[\rho(\vec{r})/\rho_{\text{hs}}(\vec{r})], \quad (19)$$

$$\begin{aligned} F_3^i &= -\frac{1}{2\beta} \int d\vec{r}_1 d\vec{r}_2 c_{\text{hs}}^{(2)}(\vec{r}_1, \vec{r}_2) [\rho(\vec{r}_1) - \rho_{\text{hs}}(\vec{r}_1)] \\ &\times [\rho(\vec{r}_2) - \rho_{\text{hs}}(\vec{r}_2)]. \end{aligned} \quad (20)$$

The counterpart of equation (18) for a homogeneous (solid or liquid) phase is

$$f_{\text{hs},r} \rho - f_{\text{hs}} \rho_{\text{hs}} = f_2 \rho + (\mu_{\text{hs}} - k_B T)(\rho - \rho_{\text{hs}}) + f_3 \rho, \quad (21)$$

and equations (19) and (20) are reduced to

$$\begin{aligned} f_2 &= k_B T \log[\rho/\rho_{\text{hs}}], \\ f_3 &= -\frac{1}{2\beta\rho} \int d\vec{r}' c_{\text{hs}}^{(2)}(\vec{r}') (\rho - \rho_{\text{hs}})^2. \end{aligned} \quad (22)$$

Notice that in the interfacial region $\int_{V_{\text{hs}}^{(i)}} d\vec{r} \rho_{\text{hs}}(\vec{r}) = (\rho_{\text{hs}}^s + \rho_{\text{hs}}^l) V_{\text{hs}}^{(i)}/2$ follows from equations (2) and (12), then a combination of equations (5), (18), (21) and (14) yields a perturbative formula for the interfacial free energy γ

$$\gamma = \gamma_{\text{hs}} + \gamma_{\text{pert}}, \quad \gamma_{\text{pert}} = \sum_{\alpha=1}^3 \gamma_{\text{pert}}^{(\alpha)}. \quad (23)$$

All the contributions $\gamma_{\text{pert}}^{(\alpha)}$ in equation (23) are given by

$$\gamma_{\text{pert}}^{(\alpha)} = \frac{F_{\alpha}^i}{A} - \frac{1}{2}(f_{\alpha}^s \rho^s + f_{\alpha}^l \rho^l) \Delta z_{\text{hs}} \quad (\alpha = 1, 2, 3), \quad (24)$$

where f_{α}^s are given by equations (10) and (22). This equation is the major result of this paper. To transform equation (24) into a form suitable for numerical calculations, F_{α}^i can be written as an integration over a local free energy density $f_{\alpha}^i(\bar{\rho}(z))$

$$F_{\alpha}^i = \int dz \bar{\rho}(z) f_{\alpha}^i(\bar{\rho}(z)), \quad (25)$$

where the detailed forms of functions $f_{\alpha}^i(\bar{\rho}(z))$ are given in appendix A.

For practical calculations the following thermodynamic properties of the HS liquid phase are used: the Carnahan–Starling free energy f_{hs}^l [41], $g_{\text{hs}}^l(r/d_l)$ of Verlet–Weis [35, 42] and $c_{\text{hs}}^{(2)l}(r)$ of Percus–Yevick [38]. For the HS solid phase, f_{hs}^s of HS fcc crystal from the fundamental measure density functional theory (FM DFT) of [45, 46] are used and the pair correlation functions $g_{\text{hs}}^s(r/d_s)$ are from the Rascon *et al* [39] parametrization. To complete this section, we note that since the HD diameters in coexisting solid d_s and liquid d_l are slightly different from each other, $d = (d_s + d_l)/2$ is used as the HS diameter of the interfacial region.

3. Results

To demonstrate the utility of the above perturbation expression for the interfacial free energy we apply this method to calculate interfacial free energies of the following model systems: inverse-power soft-spheres, the LJ model and EAM models of metallic systems.

For fcc solid–liquid systems, FM DFT is used to calculate the free energy of HS solid and liquid phases. At the coexistence of HS fcc crystal and its melt, the solid and liquid densities are $\rho^s d^3 = 1.023$ and $\rho^l d^3 = 0.934$ and the chemical potential and pressure are $\beta\mu = 15.75$ and $\beta P d^3 = 11.28$. The reference interfacial free energies of the HS fcc solid–liquid system are from [18], namely $\beta\gamma_{100}^{(\text{HS})} d^2 = 0.592$, $\beta\gamma_{110}^{(\text{HS})} d^2 = 0.571$ and $\beta\gamma_{111}^{(\text{HS})} d^2 = 0.557$.

Thermodynamic quantities of the inverse n th power repulsive system (system of soft-spheres) with the potential

$$\psi(r) = \epsilon \left(\frac{\sigma}{r} \right)^n \quad (26)$$

depend only on a single dimensionless density parameter $\rho^* = \rho \sigma'^3$, where $\sigma' = (\beta\epsilon)^{1/n} \sigma$. Figure 1 shows the comparison of γ_{100} , γ_{110} , γ_{111} between the present theory and molecular dynamics simulations [18] for different values of the parameter of inverse-power potential n . It is found that the present theoretical results differ from the MD results within 2.5%.

Next we consider a LJ system with the following potential

$$\psi(r) = 4\epsilon \left[\left(\frac{\sigma}{r} \right)^{12} - \left(\frac{\sigma}{r} \right)^6 \right]. \quad (27)$$

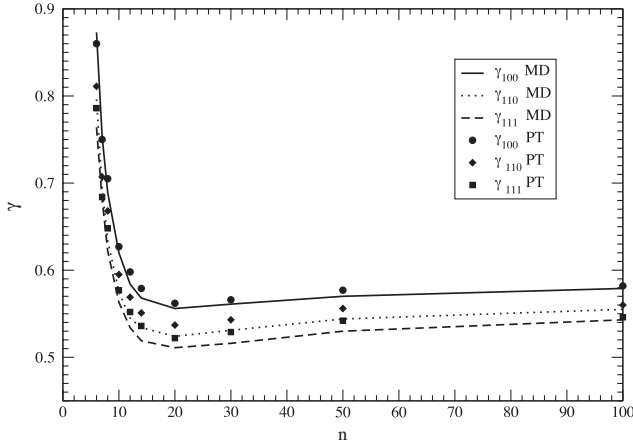


Figure 1. Solid–liquid interfacial free energy $\beta\gamma\sigma^2$ versus the soft-sphere potential n obtained from our perturbation theory (PT) and molecular dynamics simulations (MD) [18].

Table 1. Lennard-Jones solid–liquid interfacial free energy γ (in units of $\epsilon\sigma^{-2}$) for three crystal orientations and selected temperatures $T^* = k_B T/\epsilon$. The corresponding MD simulation results are taken from [19].

T^*	γ_{100}	γ_{110}	γ_{111}	$\gamma_{100}^{(MD)}$	$\gamma_{110}^{(MD)}$	$\gamma_{111}^{(MD)}$
0.617	0.408	0.400	0.392	0.371	0.360	0.347
1.0	0.596	0.577	0.564	0.562	0.543	0.508
1.5	0.879	0.844	0.822	0.84	0.82	0.75

Table 1 lists comparisons between the MD data for γ_{100} , γ_{110} , γ_{111} and theoretical values from the present work for three dimensionless temperatures $T^* = k_B T/\epsilon = 0.617$ (near triple point), 1.0 and 1.5. The present theory typically yields relative errors of γ s within 10% of the MD values at all temperatures.

Finally we consider the interfacial properties of EAM model potentials of metals. Details about the extension of our perturbation method to the case of many body potentials can be found in appendix B. We used an EAM potential of Al given by Mei and Davenport [47, 48] as an example. The obtained results for melting parameters and interfacial free energy at zero pressure are given in table 2 and compared to the ones from MD simulations [49].

In table 2 T_m is the melting temperature, l_m the enthalpy of fusion per particle, $\gamma_0 = (10\gamma_{100} + 16\gamma_{110} + 9\gamma_{111})/35$ an orientationally averaged interfacial free energy, $\epsilon_4 = (\gamma_{100} - \gamma_{110})/(\gamma_{100} + \gamma_{110})$ an anisotropy parameter and $c_T = \gamma_0/(l_m\rho_s^{2/3})$ is the Turnbull coefficient [50]. Again reasonable agreements between the results of the present theory and those of computer simulations are found.

We also computed melting and interfacial properties for the fcc phase of Fe. As a model potential of Fe we used the EAM potential given by Ackland *et al* [51]. The calculated melting properties, average interfacial free energy and anisotropy parameters at zero pressure are given in table 3. The results are compared with the MD simulation ones of Sun *et al* [23]. Table 3 Δv_{melt} shows the volume change of melting per particle and $\epsilon_1 = (35\gamma_{100} - 8\gamma_{110} - 27\gamma_{111})/22\gamma_0$ and $\epsilon_2 = 3(\gamma_{100} - 4\gamma_{110} + 3\gamma_{111})/22\gamma_0$, the anisotropy parameters

Table 2. The calculated values, related to melting and solid–liquid interfacial free energies for fcc Al at zero pressure. The EAM potential of Al is from [47, 48]. The results are compared to corresponding ones from MD simulations of Morris *et al* [49].

	Present	MDS
T_m (K)	1050	931
ρ^s (\AA^{-3})	0.056	0.056
ρ^l (\AA^{-3})	0.053	0.052
l_m (eV/atom)	0.099	0.096
γ_0 (meV \AA^{-2})	7.7	6.1
c_T	0.54	0.43
ϵ_4	0.017	0.022

Table 3. The calculated melting properties, average interfacial free energy and anisotropy parameters at zero pressure for the fcc Fe structure based upon the Fe EAM potential of Ackland *et al* [51]. The results are compared to MD simulation values of Sun *et al* [23].

	Present	MDS
l_m (eV/atom)	0.200	0.200
T_m (K)	2375	2251.0
Δv_{melt} ($\text{\AA}^3/\text{atom}$)	0.75	0.60
ρ^s (\AA^{-3})	0.0788	0.0774
c_T	0.67	0.55
γ_0 (mJ m^{-2})	378	319
ϵ_1 (%)	7.1	11.7
ϵ_2 (%)	−0.5	−0.17
$\frac{\gamma_{100} - \gamma_{110}}{2\gamma_0}$ (%)	1.4	2.8
$\frac{\gamma_{100} - \gamma_{111}}{2\gamma_0}$ (%)	2.5	3.9

of interfacial free energy. Again reasonable agreements with the results of MD simulations [23] are found.

4. Conclusions

In the present study a perturbation approach for determining solid–liquid interfacial free energies γ is developed. The approach was applied to three model systems with inverse-power, Lennard-Jones and embedded-atom model potentials. In all cases we found the magnitudes and anisotropy of γ to be in reasonable agreement with the corresponding results from MD simulations. Fundamental measure density functional theory (FM DFT) [43, 44] is used to compute thermodynamical parameters of reference HS fcc solid, which is known to give accurate phase coexistence conditions.

Besides the perturbation method, several other approximations are used in our approach. First, we assume that the width of the interface of the molecular system is the same as the width of the reference HS system, i.e. $\Delta z = \Delta z_{\text{hs}}$. Second, due to the lack of information about the correlation functions in the interfacial region, we assume that the correlation function g and direct correlation function $c^{(2)}$ are given as an interpolation of their homogeneous functions in equations (A.4), (A.10). Since the direct correlation function $c_{\text{hs}}^{(2)s}$ in a bulk solid is generally unknown and the contribution from $c_{\text{hs}}^{(2)s}$ practically does not affect the value of bulk HS solid free energy (see equation (21)), in the present study we did not account for this contribution. Finally, the number of interfacial layers,

which affects the values Δz_{hs} for the different orientations of the crystal orientations [32], could be accounted for as fitting parameters. We chose these numbers to be 5, 8, 5 for the three crystal orientations (100), (110), (111), respectively. Naturally all of the approximations can be relaxed if further information is available.

Our approach can be extended to calculate interfacial free energies of the solid–liquid mixture systems, particularly metal alloys, where the impact of the methodology can be realized. Indeed, the FM DFT can be generalized to a HS mixture, and the way to find the coexistence in a LJ mixture and EAM metal alloys using the WCA-type perturbation theory was described in [52, 53]. Some interfacial free energies $\gamma^{(\text{HS})}$ for different orientations of the crystal surface for binary mixtures are already available in [15], but more systematic studies are needed.

The method can be also applied to a bcc crystal–melt interface or other types of crystal lattices given reliable and accurate results for f_{hs}^{s} of bcc or other crystal lattices [61].

Acknowledgments

This research was sponsored by the Division of Materials Sciences and Engineering, Office of Basic Energy Sciences, US Department of Energy, under contract W-7405-ENG-82 with Iowa State University (VBW and XS) and by an NSF grant CHE-0809431(XS).

Appendix A. Functions $\{f_{\alpha}^i\}$ in equation (25)

First of all we express F_1^i in the form of equation (25), i.e.

$$F_1^i = \int dz \bar{\rho}(z) f_1^i(\bar{\rho}(z)). \quad (\text{A.1})$$

To this end we change variables the \vec{r}_1, \vec{r}_2 to $\vec{r} = \vec{r}_2 - \vec{r}_1$ and $\vec{r}' = \vec{r}_1$ in the right-hand side of equation (8) to find

$$F_1^i = \frac{1}{2} A \int \int d\vec{r} dz' \bar{\rho}(z) \bar{\rho}(z+z') \tilde{g}_{\text{hs}}(z', r) \psi_{\text{pert}}(z', r), \quad (\text{A.2})$$

where

$$\tilde{g}(z', \vec{r})_{\text{hs}} = \frac{1}{A} \int dx' dy' \frac{\rho(\vec{r}') \rho(\vec{r}' + \vec{r})}{\bar{\rho}(z') \bar{\rho}(z' + z)} g_{\text{hs}}(\vec{r}', \vec{r}). \quad (\text{A.3})$$

As no or little information is known about the two particle distribution functions in the interfacial region we approximate $\tilde{g}_{\text{hs}}(z/d, r') \psi_{\text{pert}}(z, r')$ by a simple mixing of the bulk values

$$g_{\text{hs}}\left(\frac{z}{d}, r'\right) \psi_{\text{pert}}(z, r') = g_{\text{hs}}^1\left(\frac{r'}{d_1}\right) \psi_{\text{pert}}^1(r') + \left[g_{\text{hs}}^{\text{s}}\left(\frac{r'}{d_{\text{s}}}\right) \psi_{\text{pert}}^{\text{s}}(r') - g_{\text{hs}}^1\left(\frac{r'}{d_1}\right) \psi_{\text{pert}}^1(r') \right] \Theta\left(\frac{z}{d}\right). \quad (\text{A.4})$$

Other possible ways of approximating pair correlation functions in the interfacial region are available in [54–57].

Now, using equation (A.4), we transform F_1^i in equation (A.2) to the final form of equation (A.1), where

$$f_1^i\left(\frac{z}{d}\right) = \pi \int_0^{\pi} \sin \theta' d\theta' \left\{ E_1\left(\frac{z}{d}, \theta'\right) + \left[E_{\text{s}}\left(\frac{z}{d}, \theta'\right) - E_1\left(\frac{z}{d}, \theta'\right) \right] \Theta\left(\frac{z}{d}\right) \right\}, \quad (\text{A.5})$$

$$E_{\text{s},1}\left(\frac{z}{d}, \theta'\right) = \int_0^{+\infty} r'^2 dr' \bar{\rho}\left(\frac{z+r'\cos\theta'}{d}\right) \times \tilde{g}_{\text{hs}}^{\text{s},1}\left(\frac{r'}{d_{\text{s},1}}\right) \psi_{\text{pert}}^{\text{s},1}(r'). \quad (\text{A.6})$$

Next we write F_3^i in the form of equation (25), i.e.

$$F_3^i = \int dz \bar{\rho}(z) f_3^i(\bar{\rho}(z)). \quad (\text{A.7})$$

After the transformation of equation (20) we have

$$F_3^i = \frac{1}{2} A \int \int d\vec{r} dz' \Delta \bar{\rho}(z) \Delta \bar{\rho}(z+z') \tilde{c}_{\text{hs}}^{(2)}(z', r) \quad (\text{A.8})$$

where $\Delta \bar{\rho}(z) = \bar{\rho}(z) - \bar{\rho}_{\text{hs}}(z)$ and

$$\tilde{c}^{(2)}(z', \vec{r}) = \frac{1}{A} \int dx' dy' \frac{\Delta \rho(\vec{r}') \Delta \rho(\vec{r}' + \vec{r})}{\Delta \bar{\rho}(z') \Delta \bar{\rho}(z' + z)} c_{\text{hs}}^{(2)}(\vec{r}', \vec{r}). \quad (\text{A.9})$$

Again the function $\tilde{c}^{(2)}$ in the interface region can be interpolated by the mixing of the bulk values

$$\tilde{c}_{\text{hs}}^{(2)}\left(\frac{z}{d}, r'\right) = \tilde{c}_{\text{hs}}^{(2)1}\left(\frac{r'}{d_1}\right) + \left[\tilde{c}_{\text{hs}}^{(2)\text{s}}\left(\frac{r'}{d_{\text{s}}}\right) - \tilde{c}_{\text{hs}}^{(2)1}\left(\frac{r'}{d_1}\right) \right] \Theta\left(\frac{z}{d}\right), \quad (\text{A.10})$$

although others interpolations are also available [58].

Finally, substitution of equation (A.10) into equation (A.8) yields equation (A.7), where

$$f_3^i(z) = \frac{\pi \Delta \bar{\rho}(z/d)}{\beta \bar{\rho}(z/d)} \int_0^{\pi} \sin \theta' d\theta' \left\{ H_1\left(\frac{z}{d}, \theta'\right) + \left[H_{\text{s}}\left(\frac{z}{d}, \theta'\right) - H_1\left(\frac{z}{d}, \theta'\right) \right] \Theta\left(\frac{z}{d}\right) \right\}, \quad (\text{A.11})$$

$$H_{\text{s},1}(z, \theta') = \int_0^{+\infty} r'^2 dr' \Delta \bar{\rho}\left(\frac{z+r'\cos\theta'}{d}\right) \times \tilde{c}_{\text{hs}}^{(2)\text{s},1}\left(\frac{r'}{d_{\text{s},1}}\right). \quad (\text{A.12})$$

Appendix B. Generalization of equation (23) to an EAM potential

In this part of the appendix we show how to generalize equation (23) to the case of an embedded-atom model (EAM) potential. Consider a system with interatomic interaction described by an EAM. Within this model the total energy E_{tot} is given by [59]

$$E_{\text{tot}} = \sum_k U(e_k) + \frac{1}{2} \sum_{k \neq m} \phi(r_{km}), \quad (\text{B.1})$$

where $e_k = \sum_{m \neq k} f(r_{km})$ is the total electron density at atom k due to the rest of the atoms of the system, U the embedding energy to place an atom into that electron density and ϕ is the repulsive pair interaction (r_{km} is the distance between atoms k and m). To derive an effective pair potential the function $U(e_k)$ can be replaced with a Taylor expansion about an average electron density \bar{e} [60]. It gives

$$E_{\text{tot}} = F_4 + \frac{1}{2} \sum_{k \neq m} \psi(r_{km}), \quad (\text{B.2})$$

where $\psi(r)$ is an effective (density-dependent) pair potential

$$\psi(r) = \phi(r) + U'(\bar{e})f(r) + \frac{1}{2}U''(\bar{e})[f(r)]^2 \quad (\text{B.3})$$

and F_4 is a configuration independent contribution, which is equal in the bulk to Nf_4 , where

$$f_4(\bar{e}) = U(\bar{e}) - \bar{e}U'(\bar{e}). \quad (\text{B.4})$$

In the above expressions the symbols ' and '' denote the first and second derivatives with respect to electron density. For practical calculations the average host electron density \bar{e} is approximated by the average electron density for a substitutionally disordered fcc solid solution with a lattice constant such that the overall atomic density matches the given bulk density.

To generalize equations (B.2)–(B.4) to the inhomogeneous case we assume that the electron density \bar{e} is gradually changed along the interface (along the z -direction) from \bar{e}^s to \bar{e}^l (bulk solid and liquid values, correspondingly) and can be approximated by a hyperbolic tangent expression

$$\bar{e}(z) = \bar{e}^l + [\bar{e}^s - \bar{e}^l]\Theta(z), \quad (\text{B.5})$$

where $\Theta(z)$ is given by equation (2). With such an assumption the contribution F_4 and effective pair potential ψ could be approximated by

$$F_4^i = \int dz \bar{\rho}(z) f_4^i(\bar{e}(z)) \quad (\text{B.6})$$

and

$$\psi(z_1, r) = \phi(r) + U'(\bar{e}(z_1))f(r) + \frac{1}{2}U''(\bar{e}(z_1))[f(r)]^2. \quad (\text{B.7})$$

Equations (7) and (9) now are written as $F^i = F_{\text{hs},r}^i + F_1^i + F_4^i$ and $f = f_{\text{hs},r} + f_1 + f_4$, correspondingly, with the interparticle potential given by (B.7). As a result an interfacial free energy can be calculated from equation (23) with the summation in the right-hand side running from 1 to 4, with the term $\gamma_{\text{pert}}^{(4)}$ being given by equations (24), (B.4), (B.6).

References

- [1] Morris J R and Napolitano R E 2004 *JOM* **56** 40
 [2] Hoyt J J, Asta M and Karma A 2003 *Mater. Sci. Eng.* **41** 121

- [3] Morris J R, Dahlborg U and Calvo-Dahlborg M 2007 *J. Non-Cryst. Solids* **353** 3444
 [4] Hoyt J J, Asta M, Haxhimali T, Karma A, Napolitano R E, Trivedi R, Laird B B and Morris J R 2004 *MRS Bull.* **29** 935
 [5] Gibbs J W 1948 *The Collected Works of J W Gibbs* vol 1 (New Haven, CT: Yale University Press)
 [6] Rusanov A I, Shchekin A K and Tatyanyenko D V 2009 *J. Chem. Phys.* **131** 161104
 [7] Laird B B, Davidchak R L, Yang Y and Asta M 2009 *J. Chem. Phys.* **131** 114110
 [8] Frolov T and Mishin Y 2009 *Phys. Rev. B* **79** 045430
 [9] Frolov T and Mishin Y 2009 *J. Chem. Phys.* **131** 054702
 [10] Broughton J Q and Gilmer G H 1986 *J. Chem. Phys.* **84** 5759
 [11] Davidchak R L and Laird B B 2000 *Phys. Rev. Lett.* **85** 4751
 [12] Hoyt J J, Asta M and Karma A 2001 *Phys. Rev. Lett.* **86** 5530
 [13] Mu Y, Houk A and Song X 2005 *J. Phys. Chem. B* **109** 6500
 [14] Davidchak R L, Morris J R and Laird B B 2006 *J. Chem. Phys.* **125** 094710
 [15] Amini M and Laird B B 2008 *Phys. Rev. B* **78** 144112
 [16] Mu Y and Song X 2006 *Phys. Rev. E* **74** 031611
 [17] Mu Y and Song X 2006 *J. Chem. Phys.* **124** 034712
 [18] Davidchak R L and Laird B B 2005 *Phys. Rev. Lett.* **94** 086102
 [19] Davidchak R L and Laird B B 2003 *J. Chem. Phys.* **118** 7651
 [20] Morris J R and Song X 2003 *J. Chem. Phys.* **119** 3920
 [21] Becker C A, Olmsted D, Asta M, Hoyt J J and Foiles S M 2007 *Phys. Rev. Lett.* **98** 125701
 [22] Morris J R 2002 *Phys. Rev. B* **66** 144104
 [23] Sun D Y, Asta M and Hoyt J J 2004 *Phys. Rev. B* **69** 174103
 [24] Asta M, Hoyt J J and Karma A 2002 *Phys. Rev. B* **66** 100101(R)
 [25] Handel R, Davidchak R L, Anwar J and Brukhno A 2008 *Phys. Rev. Lett.* **100** 036104
 [26] Toxvaerd S 1971 *J. Chem. Phys.* **55** 3116
 [27] Upstill C E and Evans R 1977 *J. Phys. C: Solid State Phys.* **10** 2791
 [28] Lekner J and Henderson J R 1977 *Mol. Phys.* **34** 333
 [29] Curtin W A 1989 *Phys. Rev. B* **39** 6775
 [30] Valeriani C, Wang C-Z and Frenkel D 2007 *Mol. Simul.* **33** 1023
 [31] Weeks J D, Chandler D and Andersen H C 1971 *J. Chem. Phys.* **54** 5237
 [32] Warshavsky V B and Song X 2006 *Phys. Rev. E* **73** 031110
 [33] Davidchak R L and Laird B B 1998 *J. Chem. Phys.* **108** 9452
 [34] Kang H S, Ree T and Ree F H 1986 *J. Chem. Phys.* **84** 4547
 [35] Verlet L and Weis J 1972 *Phys. Rev. A* **5** 939
 [36] Evans R 1992 *Fundamentals of Inhomogeneous Fluid* ed D Henderson (New York: Wiley)
 [37] Rascon C, Mederos L and Navascues G 1996 *Phys. Rev. Lett.* **77** 2249
 [38] Hansen J and McDonald I 1986 *Theory of Simple Liquids* 2nd edn (San Diego, CA: Academic)
 [39] Rascon C, Mederos L and Navascues G 1996 *Phys. Rev. E* **54** 1261
 [40] Rascon C, Mederos L and Navascues G 1996 *J. Chem. Phys.* **105** 10527
 [41] Carnahan N E and Starling K E 1969 *J. Chem. Phys.* **51** 635
 [42] Smith W R, Henderson D J, Leonard P J, Barker J A, Grundke E W and Henderson D 2008 *Mol. Phys.* **106** 3
 [43] Rosenfeld Y 1989 *Phys. Rev. Lett.* **63** 980
 [44] Warshavsky V B and Song X 2004 *Phys. Rev. E* **69** 061113
 [45] Roth R, Evans R, Lang A and Kahl G 2002 *J. Phys.: Condens. Matter* **14** 12063
 [46] Tarazona P 2002 *Physica A* **306** 243
 [47] Mei J and Davenport J 1992 *Phys. Rev. B* **46** 21
 [48] Sturgeon J and Laird B 2000 *Phys. Rev. B* **62** 14720
 [49] Morris J R, Mendeleev M I and Srolovitz D J 2007 *J. Non-Cryst. Solids* **353** 3565
 [50] Turnbull D 1950 *J. Appl. Phys.* **21** 1022

- [51] Ackland G J, Bacon D J, Calder A F and Harry T 1997 *Phil. Mag. A* **75** 713
- [52] Warshavsky V B and Song X 2008 *J. Chem. Phys.* **129** 034506
- [53] Warshavsky V B and Song X 2009 *Phys. Rev. B* **79** 014101
- [54] Toxvaerd S 1973 *Mol. Phys.* **26** 91
- [55] Carey B S, Scriven L E and Davis H T 1978 *J. Chem. Phys.* **69** 5040
- [56] Lekner J and Henderson J R 1980 *Mol. Phys.* **39** 1437
- [57] Davis H T and Scriven L E 1982 *Adv. Chem. Phys.* **49** 357
- [58] Iatsevitch S and Forstmann F 1997 *J. Chem. Phys.* **107** 6925
- [59] Daw M S and Baskes M L 1984 *Phys. Rev. B* **29** 6443
- [60] Foiles S M 1985 *Phys. Rev. B* **32** 3409
- [61] Warshavsky V B and Song X, in preparation